ELSEVIER

Inclusive charged hadron production in two-photon collisions at LEP

L3 Collaboration

P. Achard [t], O. Adriani [q], M. Aguilar-Benitez [x], J. Alcaraz [x,r], G. Alemanni [v], J. Allaby [r], A. Aloisio [ab], M.G. Alviggi [ab], H. Anderhub [at], V.P. Andreev [f,ag], F. Anselmo [h], A. Arefiev [aa], T. Azemoon [c], T. Aziz [i,r], P. Bagnaia [al], A. Bajo [x], G. Baksay [y], L. Baksay [y], S.V. Baldew [b], S. Banerjee [i], Sw. Banerjee [d], A. Barczyk [at,ar], R. Barillère [r], P. Bartalini [v], M. Basile [h], N. Batalova [aq], R. Battiston [af], A. Bay [v], F. Becattini [q], U. Becker [m], F. Behner [at], L. Bellucci [q], R. Berbeco [c], J. Berdugo [x], P. Berges [m], B. Bertucci [af], B.L. Betev [at], M. Biasini [af], M. Biglietti [ab], A. Biland [at], J.J. Blaising [d], S.C. Blyth [ah], G.J. Bobbink [b], A. Böhm [a], L. Boldizsar [l], B. Borgia [al], S. Bottai [q], D. Bourilkov [at], M. Bourquin [t], S. Braccini [t], J.G. Branson [an], F. Brochu [d], J.D. Burger [m], W.J. Burger [af], X.D. Cai [m], M. Capell [m], G. Cara Romeo [h], G. Carlino [ab], A. Cartacci [q], J. Casaus [x], F. Cavallari [al], N. Cavallo [ai], C. Cecchi [af], M. Cerrada [x], M. Chamizo [t], Y.H. Chang [av], M. Chemarin [w], A. Chen [av], G. Chen [g], G.M. Chen [g], H.F. Chen [u], H.S. Chen [g], G. Chiefari [ab], L. Cifarelli [am], F. Cindolo [h], I. Clare [m], R. Clare [ak], G. Coignet [d], N. Colino [x], S. Costantini [al], B. de la Cruz [x], S. Cucciarelli [af], J.A. van Dalen [ad], R. de Asmundis [ab], P. Déglon [t], J. Debreczeni [l], A. Degré [d], K. Dehmelt [y], K. Deiters [ar], D. della Volpe [ab], E. Delmeire [t], P. Denes [aj], F. DeNotaristefani [al], A. De Salvo [at], M. Diemoz [al], M. Dierckxsens [b], C. Dionisi [al], M. Dittmar [at,r], A. Doria [ab], M.T. Dova [j,5], D. Duchesneau [d], M. Duda [a], B. Echenard [t], A. Eline [r], A. El Hage [a], H. El Mamouni [w], A. Engler [ah], F.J. Eppling [m], P. Extermann [t], M.A. Falagan [x], S. Falciano [al], A. Favara [ae], J. Fay [w], O. Fedin [ag], M. Felcini [at], T. Ferguson [ah], H. Fesefeldt [a], E. Fiandrini [af], J.H. Field [t], F. Filthaut [ad], P.H. Fisher [m], W. Fisher [aj], I. Fisk [an], G. Forconi [m], K. Freudenreich [at], C. Furetta [z], Yu. Galaktionov [aa,m], S.N. Ganguli [i], P. Garcia-Abia [e,r], M. Gataullin [ae], S. Gentile [al], S. Giagu [al], Z.F. Gong [u], G. Grenier [w], O. Grimm [at], M.W. Gruenewald [p], M. Guida [am], R. van Gulik [b], V.K. Gupta [aj], A. Gurtu [i], L.J. Gutay [aq], D. Haas [e], R.Sh. Hakobyan [ad], D. Hatzifotiadou [h], T. Hebbeker [a], A. Hervé [r], J. Hirschfelder [ah], H. Hofer [at], M. Hohlmann [y], G. Holzner [at], S.R. Hou [av], Y. Hu [ad], B.N. Jin [g], L.W. Jones [c], P. de Jong [b], I. Josa-Mutuberría [x], D. Käfer [a], M. Kaur [n], M.N. Kienzle-Focacci [t], J.K. Kim [ap], J. Kirkby [r], W. Kittel [ad], A. Klimentov [m,aa],

A.C. König [ad], M. Kopal [aq], V. Koutsenko [m,aa], M. Kräber [at], R.W. Kraemer [ah],
A. Krüger [as], A. Kunin [m], P. Ladron de Guevara [x], I. Laktineh [w], G. Landi [q], M. Lebeau [r],
A. Lebedev [m], P. Lebrun [w], P. Lecomte [at], P. Lecoq [r], P. Le Coultre [at], J.M. Le Goff [r],
R. Leiste [as], M. Levtchenko [z], P. Levtchenko [ag], C. Li [u], S. Likhoded [as], C.H. Lin [av],
W.T. Lin [av], F.L. Linde [b], L. Lista [ab], Z.A. Liu [g], W. Lohmann [as], E. Longo [al], Y.S. Lu [g],
C. Luci [al], L. Luminari [al], W. Lustermann [at], W.G. Ma [u], L. Malgeri [t], A. Malinin [aa],
C. Maña [x], D. Mangeol [ad], J. Mans [aj], J.P. Martin [w], F. Marzano [al], K. Mazumdar [i],
R.R. McNeil [f], S. Mele [r,ab], L. Merola [ab], M. Meschini [q], W.J. Metzger [ad], A. Mihul [k],
H. Milcent [r], G. Mirabelli [al], J. Mnich [a], G.B. Mohanty [i], G.S. Muanza [w], A.J.M. Muijs [b],
B. Musicar [an], M. Musy [al], S. Nagy [o], S. Natale [t], M. Napolitano [ab], F. Nessi-Tedaldi [at],
H. Newman [ae], A. Nisati [al], H. Nowak [as], R. Ofierzynski [at], G. Organtini [al], C. Palomares [r],
P. Paolucci [ab], R. Paramatti [al], G. Passaleva [q], S. Patricelli [ab], T. Paul [j], M. Pauluzzi [af],
C. Paus [m], F. Pauss [at], M. Pedace [al], S. Pensotti [z], D. Perret-Gallix [d], B. Petersen [ad],
D. Piccolo [ab], F. Pierella [h], M. Pioppi [af], P.A. Piroué [aj], E. Pistolesi [z], V. Plyaskin [aa],
M. Pohl [t], V. Pojidaev [q], J. Pothier [r], D.O. Prokofiev [aq], D. Prokofiev [ag], J. Quartieri [am],
G. Rahal-Callot [at], M.A. Rahaman [i], P. Raics [o], N. Raja [i], R. Ramelli [at], P.G. Rancoita [z],
R. Ranieri [q], A. Raspereza [as], P. Razis [ac], D. Ren [at], M. Rescigno [al], S. Reucroft [j],
S. Riemann [as], K. Riles [c], B.P. Roe [c], L. Romero [x], A. Rosca [as], S. Rosier-Lees [d],
S. Roth [a], C. Rosenbleck [a], B. Roux [ad], J.A. Rubio [r], G. Ruggiero [q], H. Rykaczewski [at],
A. Sakharov [at], S. Saremi [f], S. Sarkar [al], J. Salicio [r], E. Sanchez [x], M.P. Sanders [ad],
C. Schäfer [r], V. Schegelsky [ag], H. Schopper [au], D.J. Schotanus [ad], C. Sciacca [ab],
L. Servoli [af], S. Shevchenko [ae], N. Shivarov [ao], V. Shoutko [m], E. Shumilov [aa],
A. Shvorob [ae], D. Son [ap], C. Souga [w], P. Spillantini [q], M. Steuer [m], D.P. Stickland [aj],
B. Stoyanov [ao], A. Straessner [r], K. Sudhakar [i], G. Sultanov [ao], L.Z. Sun [u], S. Sushkov [a],
H. Suter [at], J.D. Swain [j], Z. Szillasi [y,3], X.W. Tang [g], P. Tarjan [o], L. Tauscher [e],
L. Taylor [j], B. Tellili [w], D. Teyssier [w], C. Timmermans [ad], Samuel C.C. Ting [m],
S.M. Ting [m], S.C. Tonwar [i,r], J. Tóth [l], C. Tully [aj], K.L. Tung [g], J. Ulbricht [at], E. Valente [al],
R.T. Van de Walle [ad], R. Vasquez [aq], V. Veszpremi [y], G. Vesztergombi [l], I. Vetlitsky [aa],
D. Vicinanza [am], G. Viertel [at], S. Villa [ak], M. Vivargent [d], S. Vlachos [e], I. Vodopianov [ag],
H. Vogel [ah], H. Vogt [as], I. Vorobiev [ah,aa], A.A. Vorobyov [ag], M. Wadhwa [e], X.L. Wang [u],
Z.M. Wang [u], M. Weber [a], P. Wienemann [a], H. Wilkens [ad], S. Wynhoff [aj], L. Xia [ae],
Z.Z. Xu [u], J. Yamamoto [c], B.Z. Yang [u], C.G. Yang [g], H.J. Yang [c], M. Yang [g], S.C. Yeh [aw],
An. Zalite [ag], Yu. Zalite [ag], Z.P. Zhang [u], J. Zhao [u], G.Y. Zhu [g], R.Y. Zhu [ae],
H.L. Zhuang [g], A. Zichichi [h,r,s], B. Zimmermann [at], M. Zöller [a]

[a] *III Physikalisches Institut, RWTH, D-52056 Aachen, Germany* [1]
[b] *National Institute for High Energy Physics, NIKHEF, and University of Amsterdam, NL-1009 DB Amsterdam, The Netherlands*
[c] *University of Michigan, Ann Arbor, MI 48109, USA*
[d] *Laboratoire d'Annecy-le-Vieux de Physique des Particules, LAPP, IN2P3-CNRS, BP 110, F-74941 Annecy-le-Vieux cedex, France*
[e] *Institute of Physics, University of Basel, CH-4056 Basel, Switzerland*

[f] *Louisiana State University, Baton Rouge, LA 70803, USA*
[g] *Institute of High Energy Physics, IHEP, 100039 Beijing, PR China* [6]
[h] *University of Bologna, and INFN, Sezione di Bologna, I-40126 Bologna, Italy*
[i] *Tata Institute of Fundamental Research, Mumbai (Bombay) 400 005, India*
[j] *Northeastern University, Boston, MA 02115, USA*
[k] *Institute of Atomic Physics and University of Bucharest, R-76900 Bucharest, Romania*
[l] *Central Research Institute for Physics of the Hungarian Academy of Sciences, H-1525 Budapest 114, Hungary* [2]
[m] *Massachusetts Institute of Technology, Cambridge, MA 02139, USA*
[n] *Panjab University, Chandigarh 160 014, India*
[o] *KLTE-ATOMKI, H-4010 Debrecen, Hungary* [3]
[p] *Department of Experimental Physics, University College Dublin, Belfield, Dublin 4, Ireland*
[q] *INFN, Sezione di Firenze, and University of Florence, I-50125 Florence, Italy*
[r] *European Laboratory for Particle Physics, CERN, CH-1211 Geneva 23, Switzerland*
[s] *World Laboratory, FBLJA Project, CH-1211 Geneva 23, Switzerland*
[t] *University of Geneva, CH-1211 Geneva 4, Switzerland*
[u] *Chinese University of Science and Technology, USTC, Hefei, Anhui 230 029, PR China* [6]
[v] *University of Lausanne, CH-1015 Lausanne, Switzerland*
[w] *Institut de Physique Nucléaire de Lyon, IN2P3-CNRS, Université Claude Bernard, F-69622 Villeurbanne, France*
[x] *Centro de Investigaciones Energéticas, Medioambientales y Tecnológicas, CIEMAT, E-28040 Madrid, Spain* [4]
[y] *Florida Institute of Technology, Melbourne, FL 32901, USA*
[z] *INFN, Sezione di Milano, I-20133 Milan, Italy*
[aa] *Institute of Theoretical and Experimental Physics, ITEP, Moscow, Russia*
[ab] *INFN, Sezione di Napoli, and University of Naples, I-80125 Naples, Italy*
[ac] *Department of Physics, University of Cyprus, Nicosia, Cyprus*
[ad] *University of Nijmegen and NIKHEF, NL-6525 ED Nijmegen, The Netherlands*
[ae] *California Institute of Technology, Pasadena, CA 91125, USA*
[af] *INFN, Sezione di Perugia, and Università Degli Studi di Perugia, I-06100 Perugia, Italy*
[ag] *Nuclear Physics Institute, St. Petersburg, Russia*
[ah] *Carnegie Mellon University, Pittsburgh, PA 15213, USA*
[ai] *INFN, Sezione di Napoli, and University of Potenza, I-85100 Potenza, Italy*
[aj] *Princeton University, Princeton, NJ 08544, USA*
[ak] *University of Californa, Riverside, CA 92521, USA*
[al] *INFN, Sezione di Roma, and University of Rome "La Sapienza", I-00185 Rome, Italy*
[am] *University and INFN, Salerno, I-84100 Salerno, Italy*
[an] *University of California, San Diego, CA 92093, USA*
[ao] *Bulgarian Academy of Sciences, Central Lab. of Mechatronics and Instrumentation, BU-1113 Sofia, Bulgaria*
[ap] *The Center for High Energy Physics, Kyungpook National University, 702-701 Taegu, South Korea*
[aq] *Purdue University, West Lafayette, IN 47907, USA*
[ar] *Paul Scherrer Institut, PSI, CH-5232 Villigen, Switzerland*
[as] *DESY, D-15738 Zeuthen, Germany*
[at] *Eidgenössische Technische Hochschule, ETH Zürich, CH-8093 Zürich, Switzerland*
[au] *University of Hamburg, D-22761 Hamburg, Germany*
[av] *National Central University, Chung-Li, Taiwan, ROC*
[aw] *Department of Physics, National Tsing Hua University, Taiwan, ROC*

Abstract

Inclusive charged hadron production, $e^+e^- \to e^+e^-h^\pm X$, is studied using 414 pb^{-1} of data collected at LEP with the L3 detector at centre-of-mass energies between 189 and 202 GeV. Single particle inclusive differential cross sections are measured as a function of the particle transverse momentum, p_t, and pseudo-rapidity, η. For $p_t \leqslant 1.5$ GeV, the data are well described by

an exponential, typical of soft hadronic processes. For higher p_t, the onset of perturbative QCD processes is observed. The $\pi^{\pm}$ production cross section for $p_t > 5$ GeV is much higher than the NLO QCD predictions.

1. Introduction

Two-photon collisions are the main source of hadron production in the high-energy regime of LEP via the process $e^+e^- \rightarrow e^+e^-\gamma^*\gamma^* \rightarrow e^+e^-$ hadrons. In the Vector Dominance Model (VDM), each photon can transform into a vector meson with the same quantum numbers, thus initiating a strong interaction process with characteristics similar to hadron–hadron interactions. This process dominates in the "soft" interaction region, where hadrons are produced with a low transverse momentum, p_t, with respect to the beam direction. Hadrons with high p_t are produced by the direct QED process $\gamma^*\gamma^* \rightarrow q\bar{q}$ or by QCD processes originating from the partonic content of the photon. QCD calculations are available for single particle inclusive production in two-photon interactions at next-to-leading order (NLO) precision [1,2].

The L3 Collaboration recently published results on inclusive π^0 and K_S^0 production [3]. The π^0 differential cross section measured as a function of p_t exhibits a clear excess over QCD calculations. A comparison of these results with other single particle inclusive production at high p_t is therefore important. In this Letter, the inclusive charged hadron production is studied for a centre-of-mass energy of the two interacting photons, $W_{\gamma\gamma}$, greater than 5 GeV. The hadrons are measured in the transverse momentum range $0.4 \text{ GeV} \leqslant p_t \leqslant 20 \text{ GeV}$ and in the pseudo-rapidity[7] interval $|\eta| \leqslant 1$. The contributions from $\pi^{\pm}$ and $K^{\pm}$ are also derived.

The data used for this analysis were collected by the L3 detector [4] at centre-of-mass energies $\sqrt{s} = 189$–202 GeV, with a luminosity weighted average value of $\sqrt{s} = 194$ GeV, for an integrated luminosity of 414 pb^{-1}. Results on inclusive charged hadron production for a smaller data sample at lower $\sqrt{s}$ were previously reported [5].

The process $e^+e^- \rightarrow e^+e^-$ hadrons is modelled with the PYTHIA [6] event generator for an event sample three times larger than the data. In this generator, each photon can interact as a point-like particle, as a vector meson or as a resolved photon, leading to six classes of events. The fragmentation is simulated with JETSET. Predictions from the PHOJET Monte Carlo program [7] are also compared with the data. The following Monte Carlo generators are used to simulate the relevant background processes: KK2f [8] for $e^+e^- \rightarrow q\bar{q}(\gamma)$; KORALZ [9] for $e^+e^- \rightarrow \tau^+\tau^-(\gamma)$; KORALW [10] for $e^+e^- \rightarrow W^+W^-$ and DIAG36 [11] for $e^+e^- \rightarrow e^+e^-\tau^+\tau^-$. Events are simulated in the L3 detector using the GEANT [12] and GHEISHA [13] programs and passed through the same reconstruction program as the data. Time-dependent detector inefficiencies, as monitored during each data taking period, are also simulated.

2. Event and charged hadron selection

Two-photon events are collected predominantly by the track triggers [14] with a low p_t threshold of about 150 MeV. The selection of $e^+e^- \rightarrow e^+e^-$ hadrons events [15] consists of:

- A multiplicity cut. To select hadronic final states, at least six objects must be detected, where an

---

---

[7] $\eta = -\ln\tan(\theta/2)$, where θ is the polar angle of the particle relative to the beam axis.

object can be a track or a calorimetric cluster with no associated track.

- Energy cuts. The total energy deposited in the calorimeters must be less than $0.4\sqrt{s}$, in order to exclude e^+e^- annihilation events. The total energy in the electromagnetic calorimeter is required to be greater than 500 MeV, to suppress beam-gas and beam-wall backgrounds.
- An anti-tag condition. Events with a cluster in the luminosity monitor with an energy greater than 30 GeV and an electromagnetic shower shape are excluded.
- A mass cut. The visible mass of the event must be greater than 5 GeV.

About 2 million hadronic events are selected by these criteria. The overall background level is less than 1% and is mainly due to the $e^+e^- \to q\bar{q}(\gamma)$ and $e^+e^- \to e^+e^-\tau^+\tau^-$ processes.

Charged hadrons are measured with high quality tracks in the inner tracking detector. These tracks have a transverse momentum greater than 400 MeV and a distance of closest approach to the primary vertex in the transverse plane less than 4 mm. The number of hits must be greater than 80% of that expected from the track length. Tracks are analysed in the $|\eta| < 1$ and $p_t < 20$ GeV range where the detector resolution is optimal. A resolution $\sigma_{p_t}/p_t \simeq (0.015\,\text{GeV}^{-1})\,p_t$ is achieved.

3. Differential cross section

The differential cross sections of inclusive charged hadron production as a function of p_t are measured for an effective mass of the $\gamma\gamma$ system $W_{\gamma\gamma} \geqslant 5$ GeV, with a mean value of $\langle W_{\gamma\gamma} \rangle \simeq 30$ GeV, a photon virtuality $Q^2 \leqslant 8$ GeV^2 and an average photon virtuality $\langle Q^2 \rangle \simeq 0.2$ GeV^2. This phase space is defined by cuts at the Monte Carlo generator level. Results are presented in 12 p_t bins between 0.4 and 20 GeV.

The distribution of the detected charged hadrons in these p_t bins is presented in Fig. 1(a). The background remains very low over the whole p_t range. Events
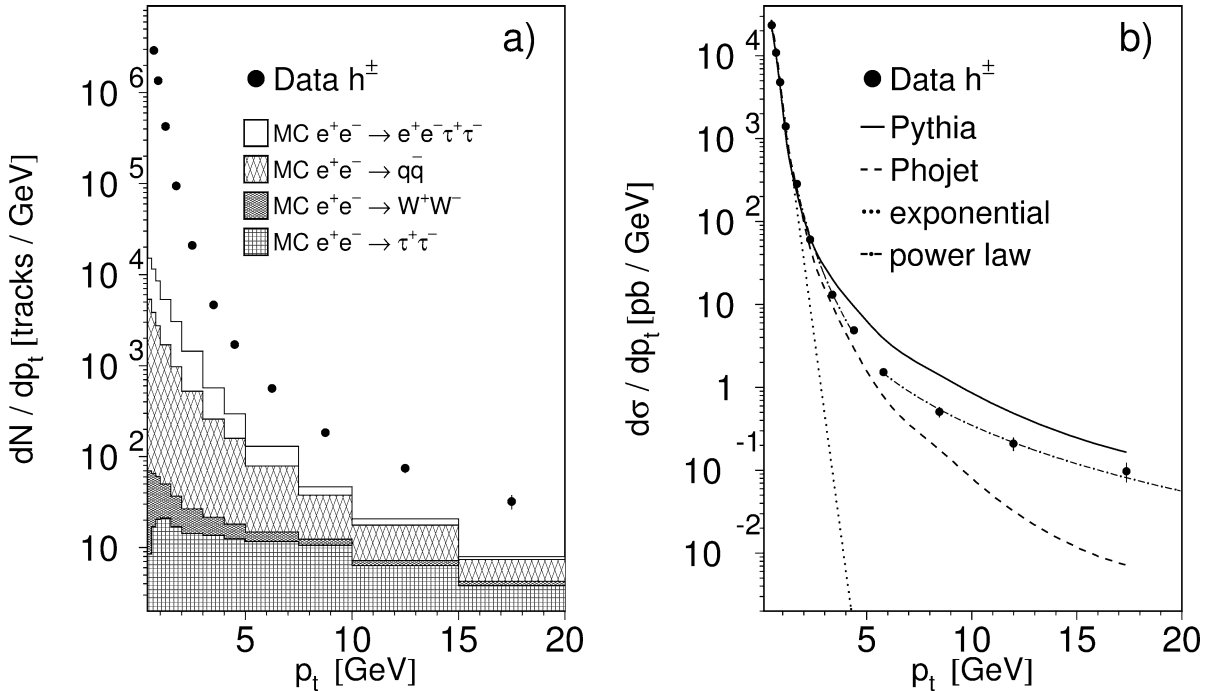

Fig. 1. (a) Number of selected tracks per GeV in each p_t bin and main sources of background. (b) Inclusive charged hadron differential cross section $d\sigma/dp_t$ fitted with an exponential and power-law functions. Monte Carlo predictions are also presented. Statistical and systematic uncertainties are shown. The average p_t value of each bin, $\langle p_t \rangle$, is used.

Table 1

Transverse momentum range and average value from the data with the corresponding overall efficiency and differential cross section for inclusive charged hadron production for $W_{\gamma\gamma} > 5$ GeV and $|\eta| < 1$. The uncertainty on the efficiency is systematic. The first uncertainty on the cross section is statistical and the second systematic

p_t [GeV]	$\langle p_t \rangle$ [GeV]	Efficiency [%]	$d\sigma/dp_t$ [pb/GeV]
0.4– 0.6	0.48	62.4 ± 7.7	$(23.4 \pm 0.1 \pm 3.7) \times 10^3$
0.6– 0.8	0.68	64.5 ± 6.9	$(10.9 \pm 0.1 \pm 1.5) \times 10^3$
0.8– 1.0	0.88	67.7 ± 6.0	$(48.0 \pm 0.1 \pm 5.9) \times 10^2$
1.0– 1.5	1.14	72.4 ± 4.8	$(14.1 \pm 0.1 \pm 1.4) \times 10^2$
1.5– 2.0	1.68	77.4 ± 3.7	$(28.5 \pm 0.1 \pm 2.2) \times 10$
2.0– 3.0	2.31	77.2 ± 4.3	$(60.9 \pm 0.5 \pm 4.4)$
3.0– 4.0	3.36	75.0 ± 5.2	$(13.1 \pm 0.2 \pm 1.0)$
4.0– 5.0	4.39	69.5 ± 5.8	$(48.7 \pm 1.3 \pm 4.2) \times 10^{-1}$
5.0– 7.5	5.79	68.1 ± 6.8	$(15.3 \pm 0.4 \pm 1.6) \times 10^{-1}$
7.5–10.0	8.46	65.2 ± 8.7	$(50.9 \pm 2.5 \pm 7.0) \times 10^{-2}$
10.0–15.0	11.98	61.9 ± 11.0	$(21.0 \pm 1.2 \pm 3.8) \times 10^{-2}$
15.0–20.0	17.36	59.8 ± 14.7	$(97.1 \pm 8.4 \pm 24.3) \times 10^{-3}$

Table 2

Systematic uncertainty on the charged hadron cross section due to trigger efficiency, background subtraction, selection procedure and Monte Carlo modeling

p_t [GeV]	Trigger efficiency [%]	Background subtraction [%]	Selection procedure [%]	Monte Carlo modeling [%]
0.4– 0.6	0.1	< 0.1	10.1	12.4
0.6– 0.8	0.1	< 0.1	9.2	10.6
0.8– 1.0	0.2	< 0.1	8.4	8.9
1.0– 1.5	0.2	< 0.1	7.5	6.6
1.5– 2.0	0.4	< 0.1	5.9	4.8
2.0– 3.0	0.5	0.1	4.5	5.6
3.0– 4.0	0.9	0.4	3.1	6.9
4.0– 5.0	1.2	0.9	2.3	8.2
5.0– 7.5	1.2	1.3	1.6	10.0
7.5–10.0	1.2	2.5	1.2	13.3
10.0–15.0	1.2	3.1	1.1	17.8
15.0–20.0	1.2	4.2	1.1	24.6

from the $e^+e^- \rightarrow e^+e^-\tau^+\tau^-$ process dominate the background at low p_t while annihilation events dominate it at high p_t. To measure the cross section, the background is subtracted bin-by-bin and the data are corrected for the selection efficiency, including acceptance, calculated bin-by-bin with PYTHIA. This selection efficiency varies from 62% to 84%. At low p_t, the efficiency decreases due to the effect of the mass and energy cuts. At high p_t, it decreases because of the multiplicity cut, since high p_t particles are mainly produced in low multiplicity events.

The level 1 trigger efficiency is obtained by comparing the number of events accepted by the independent track and calorimetric energy [16] triggers. It

varies from 95% to 98%. The efficiency of higher level triggers is about 95% and is measured using prescaled events. The overall efficiency, taking into account selection and trigger efficiencies is given in Table 1.

Sources of systematic uncertainties on the cross section measurements are the trigger efficiency estimation, the background subtraction, the selection procedure and the Monte Carlo modeling. Their contributions are shown in Table 2. The uncertainty on the trigger efficiency and on the background subtraction are of a statistical nature. The uncertainty due to the selection procedure is evaluated by repeating the analysis with different selection criteria: the multiplicity cut is moved from 5 to 7 objects, the energy cut is moved to

0.35 $\sqrt{s}$ and the number of hits of the tracks is moved to 70% of that expected. The sum in quadrature of the differences between these and the reference results is listed in Table 2. Varying other criteria give negligible contributions. To evaluate the uncertainty on the Monte Carlo modeling, the selection efficiency is determined using only one of the PYTHIA subprocesses: VDM–VDM, direct–direct or resolved–resolved. The systematic uncertainty is assigned as the average difference between these values and the reference Monte Carlo. The larger contribution comes from the difference between direct and other processes.

The differential cross section of charged hadron production as a function of p_t is presented in Fig. 1(b) and in Table 1. The migration due to the p_t resolution does not affect these results. This was verified by performing a one-step Bayesian unfolding [17] of the track p_t distribution which give results compatible, within errors, with those obtained using the bin-by-bin correction.

The steep decrease of $d\sigma/dp_t$ in the range $0.4 < p_t < 1.5$ GeV is described by an exponential of the form $A\exp(-p_t/\langle p_t \rangle)$ with a mean value of $\langle p_t \rangle \simeq 232$ MeV. This behaviour is characteristic of hadrons produced by soft interactions and is similar to that obtained in hadron–hadron and photon–hadron collisions [18]. At higher p_t the differential cross section is better represented by power law functions $A p_t^{-B}$, as expected by the onset of QCD processes. For 1.5 GeV $< p_t < 5$ GeV, $B \simeq 4.2$ and for 5 GeV $< p_t < 20$ GeV, $B \simeq 2.6$. The results of the fits are drawn on Fig. 1(b) where the data are also compared to Monte Carlo predictions. PYTHIA is slightly above the data, whereas PHOJET is too low by more than one order of magnitude. These results are consistent with our findings in inclusive π^0 production [3].

4. Charged pions and charged kaons

Assuming the fragmentation function implemented in JETSET are correct, the $\pi^{\pm}$ and the K$^{\pm}$ inclusive
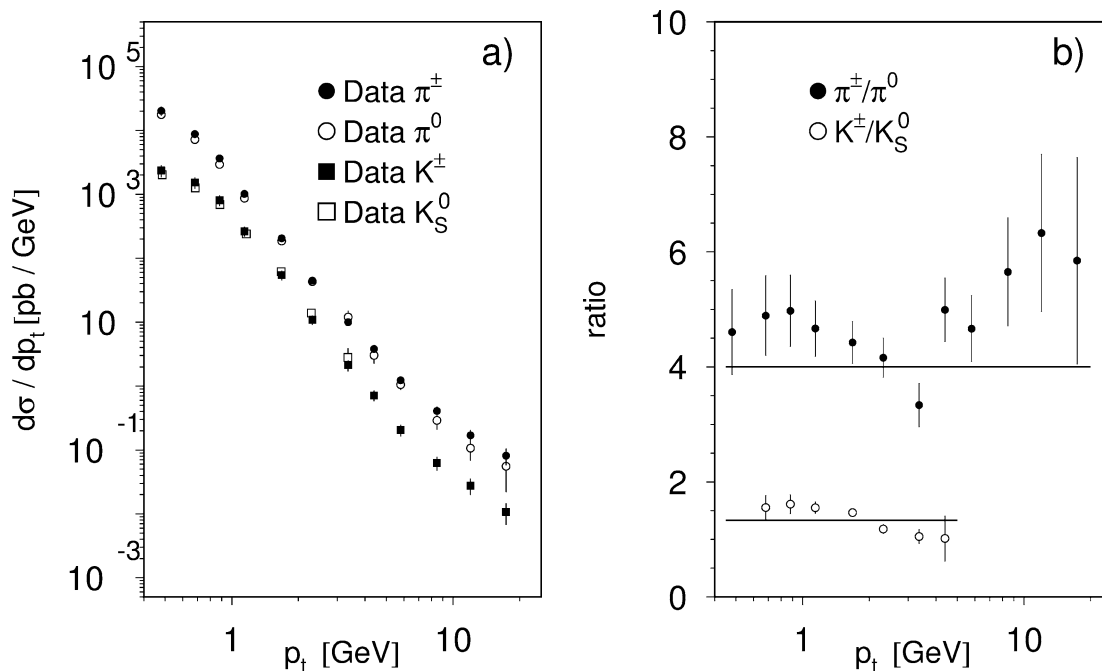

Fig. 2. (a) Differential cross section $d\sigma/dp_t$ for inclusive pion and kaon production. The $\pi^{\pm}$ data are compared to the inclusive π^0 measurement [3] scaled by a factor 4. The K$^{\pm}$ data are compared to the inclusive K$_S^0$ measurement [3] scaled by a factor 4/3. (b) Cross section ratios for pions and kaons. Good agreement is found with the expected values (horizontal lines). Statistical and systematic uncertainties are shown. The average p_t value of each bin, $\langle p_t \rangle$, is used.

Table 3
Differential cross section as a function of p_t for inclusive $\pi^\pm$ and $K^\pm$ production for $W_{\gamma\gamma} > 5$ GeV and $|\eta| < 1$. The first uncertainty on the cross section is statistical and the second systematic

$\langle p_t \rangle$ [GeV]	$d\sigma/dp_t$ for pions [pb/GeV]	$d\sigma/dp_t$ for kaons [pb/GeV]
0.48	$(20.3 \pm 0.1 \pm 3.3) \times 10^3$	$(23.7 \pm 0.1 \pm 5.1) \times 10^2$
0.68	$(88.1 \pm 0.1 \pm 12.5) \times 10^2$	$(15.3 \pm 0.1 \pm 3.1) \times 10^2$
0.88	$(36.5 \pm 0.1 \pm 4.5) \times 10^2$	$(80.7 \pm 0.2 \pm 15.3) \times 10$
1.14	$(10.2 \pm 0.1 \pm 1.0) \times 10^2$	$(26.4 \pm 0.1 \pm 4.7) \times 10$
1.68	$(20.5 \pm 0.1 \pm 1.6) \times 10$	$(54.3 \pm 0.4 \pm 9.2)$
2.31	$(44.7 \pm 0.3 \pm 3.5)$	$(10.9 \pm 0.1 \pm 1.9)$
3.36	$(10.0 \pm 0.2 \pm 0.9)$	$(21.3 \pm 0.4 \pm 3.8) \times 10^{-1}$
4.39	$(37.8 \pm 1.0 \pm 3.6) \times 10^{-1}$	$(71.3 \pm 2.4 \pm 13.4) \times 10^{-2}$
5.79	$(12.3 \pm 0.4 \pm 1.4) \times 10^{-1}$	$(20.6 \pm 0.8 \pm 4.2) \times 10^{-2}$
8.46	$(41.0 \pm 2.1 \pm 6.2) \times 10^{-2}$	$(62.9 \pm 4.1 \pm 14.8) \times 10^{-3}$
11.98	$(16.9 \pm 1.0 \pm 3.4) \times 10^{-2}$	$(27.7 \pm 2.1 \pm 7.7) \times 10^{-3}$
17.36	$(81.3 \pm 7.1 \pm 22.5) \times 10^{-3}$	$(10.7 \pm 1.4 \pm 3.7) \times 10^{-3}$

cross sections are extracted from the charged hadron cross section. Their ratios relative to charged hadrons are estimated bin-by-bin from Monte Carlo. Above 5 GeV, they are almost constant. Their uncertainty is calculated in the same way as the uncertainty on the Monte Carlo modeling of the selection efficiency, by using different subprocesses in PYTHIA. This gives an additional systematic uncertainty of from 2% to 12% for pions and from 14% to 24% for kaons.

The differential cross sections for $\pi^\pm$ and $K^\pm$ production as a function of p_t are presented in Fig. 2 and in Table 3. The $\pi^\pm$ data are compared to the previous π^0 data [3] scaled up by a factor 4: a factor 2 to correct for the $|\eta| < 0.5$ interval used for the π^0 measurement and a factor 2 to take into account the isospin symmetry. A good agreement is found between these two measurements as shown in Fig. 2. The $K^\pm$ data are compared to the previous results of K^0_S data [3] scaled up by a factor 4/3: a factor 2/3 to correct for the $|\eta| < 1.5$ interval of the K^0_S measurement and a factor 2 to take into account unobserved K^0_L decays. Good agreement is found between these two measurements as shown in Fig. 2. These agreements show a good consistency with the data of the fragmentation functions as implemented in JETSET.

The differential cross section of $\pi^\pm$ production as a function of $|\eta|$ for $p_t > 1$ GeV is shown in Fig. 3 and in Table 5. The cross section is almost constant in this η range. It agrees well with the π^0 measurement [3]. For different p_t cuts, Monte Carlo
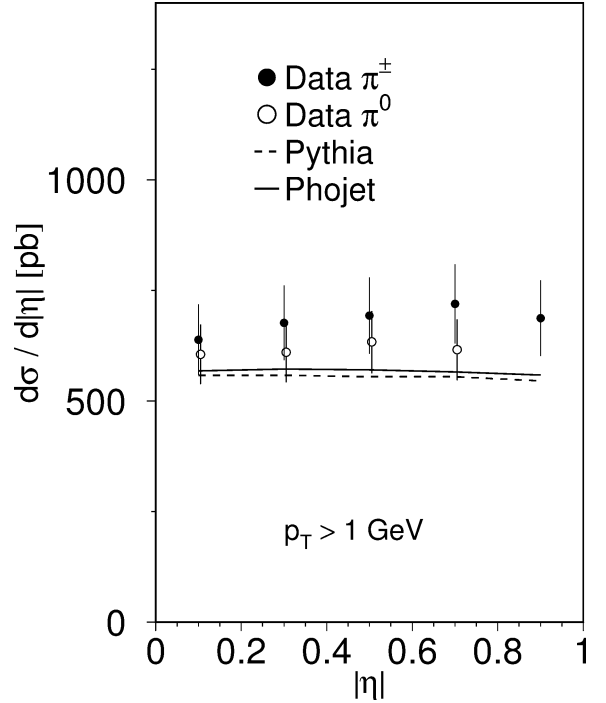

Fig. 3. Inclusive $\pi^\pm$ differential cross section $d\sigma/d|\eta|$ for $p_t > 1$ GeV compared to the inclusive π^0 measurement [3] called by a factor 2 and two Monte Carlo predictions. Statistical and systematic uncertainties are shown.

and QCD predictions describe well the uniform η distribution, while the agreement in the absolute rate depends on the p_t range considered.
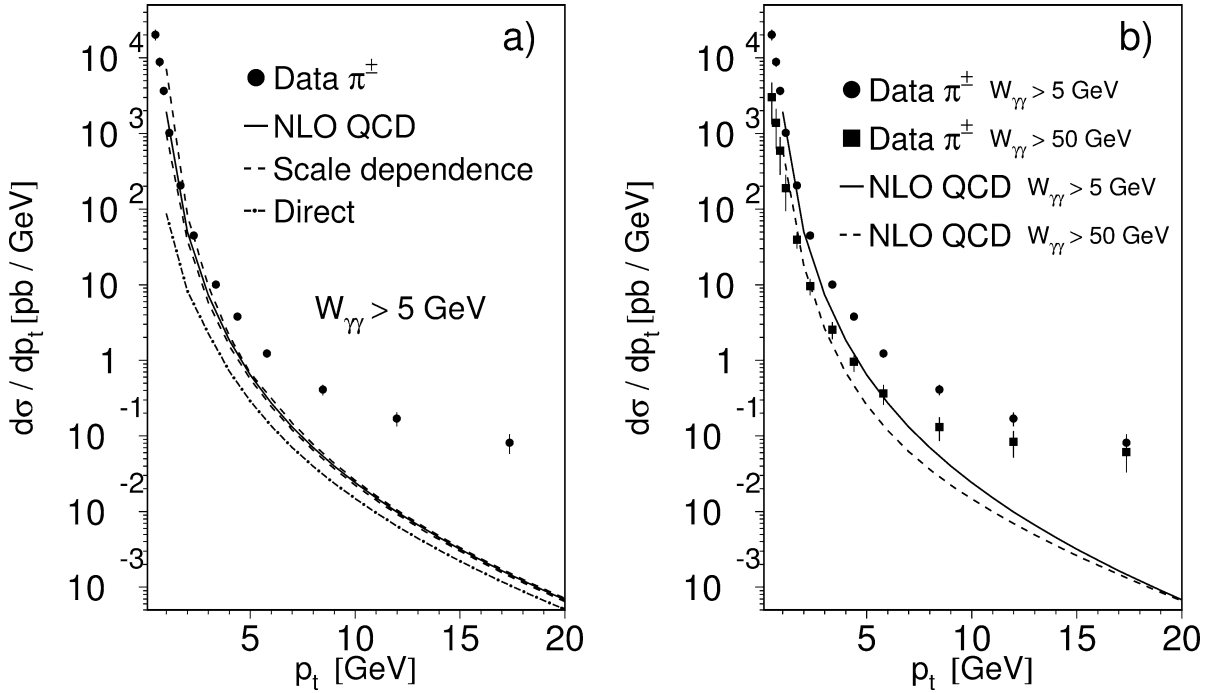
Fig. 4. (a) Inclusive $\pi^{\pm}$ differential cross section $d\sigma/dp_t$ compared to NLO QCD calculations [19] for $W_{\gamma\gamma} > 5$ GeV. The dashed-dotted line corresponds to the direct subprocess. The dashed lines represent the scale uncertainty of the calculations. (b) Inclusive $\pi^{\pm}$ differential cross section $d\sigma/dp_t$ with different $W_{\gamma\gamma}$ cuts. The average p_t value of each bin, $\langle p_t \rangle$, is used.

Table 4

Differential cross section as a function of p_t for inclusive $\pi^{\pm}$ production for $|\eta| < 1$ and different $W_{\gamma\gamma}$ cuts. The first uncertainty on the cross section is statistical and the second systematic

$\langle p_t \rangle$ [GeV]	$d\sigma/dp_t$ [pb/GeV] $W_{\gamma\gamma} > 10$ GeV	$d\sigma/dp_t$ [pb/GeV] $W_{\gamma\gamma} > 30$ GeV	$d\sigma/dp_t$ [pb/GeV] $W_{\gamma\gamma} > 50$ GeV
0.48	$(13.7 \pm 0.1 \pm 3.2) \times 10^3$	$(56.2 \pm 0.2 \pm 23.8) \times 10^2$	$(30.1 \pm 0.2 \pm 17.0) \times 10^2$
0.68	$(60.6 \pm 0.1 \pm 12.5) \times 10^2$	$(25.3 \pm 0.1 \pm 9.9) \times 10^2$	$(13.8 \pm 0.1 \pm 7.5) \times 10^2$
0.88	$(25.7 \pm 0.1 \pm 4.5) \times 10^2$	$(10.9 \pm 0.1 \pm 3.9) \times 10^2$	$(59.3 \pm 0.6 \pm 31.2) \times 10$
1.14	$(74.3 \pm 0.2 \pm 10.3) \times 10$	$(33.5 \pm 0.2 \pm 10.7) \times 10$	$(18.9 \pm 0.2 \pm 9.5) \times 10$
1.68	$(15.6 \pm 0.1 \pm 1.0) \times 10$	$(73.5 \pm 0.8 \pm 9.4)$	
2.31	$(36.4 \pm 0.3 \pm 2.2)$	$(17.2 \pm 0.3 \pm 2.0)$	$(96.1 \pm 2.3 \pm 23.4) \times 10^{-1}$
3.36	$(88.8 \pm 1.5 \pm 5.8) \times 10^{-1}$	$(40.5 \pm 1.1 \pm 4.6) \times 10^{-1}$	$(25.5 \pm 1.1 \pm 6.5) \times 10^{-1}$
4.39	$(35.7 \pm 1.0 \pm 2.9) \times 10^{-1}$	$(18.9 \pm 0.8 \pm 2.2) \times 10^{-1}$	$(96.5 \pm 6.0 \pm 26.0) \times 10^{-2}$
5.79	$(11.7 \pm 0.4 \pm 1.2) \times 10^{-1}$	$(60.4 \pm 2.5 \pm 7.2) \times 10^{-2}$	$(36.5 \pm 2.1 \pm 10.5) \times 10^{-2}$
8.46	$(37.8 \pm 2.0 \pm 5.6) \times 10^{-2}$	$(22.1 \pm 1.5 \pm 2.9) \times 10^{-2}$	$(13.1 \pm 1.2 \pm 4.4) \times 10^{-2}$
11.98	$(16.4 \pm 1.0 \pm 3.4) \times 10^{-2}$	$(12.7 \pm 0.9 \pm 1.8) \times 10^{-2}$	$(84.1 \pm 7.4 \pm 31.5) \times 10^{-3}$
17.36	$(78.9 \pm 7.0 \pm 23.9) \times 10^{-3}$	$(60.0 \pm 6.3 \pm 10.1) \times 10^{-3}$	$(61.3 \pm 7.5 \pm 27.2) \times 10^{-3}$

In Fig. 4(a) the data are compared to analytical NLO QCD predictions [2,19]. For this calculation, the flux of quasi-real photons is obtained using the Equivalent Photon Approximation [20], taking into account both transverse and longitudinal virtual photons.

The interacting particles can be point-like photons or partons from the $\gamma \to q\bar{q}$ process, which evolve into quarks and gluons. The NLO parton density functions of Ref. [21] are used and all elementary $2 \to 2$ and $2 \to 3$ processes are considered. New NLO fragmen-

Table 5
Differential cross section as a function of $|\eta|$ for inclusive $\pi^{\pm}$ production for $W_{\gamma\gamma} > 5$ GeV and $p_t > 1$ GeV. The first uncertainty on the cross section is statistical and the second systematic

$|\eta|$	$d\sigma/d|\eta|$ [pb]
0.0–0.2	$638 \pm 3 \pm 80$
0.2–0.4	$677 \pm 3 \pm 84$
0.4–0.6	$693 \pm 4 \pm 86$
0.6–0.8	$719 \pm 4 \pm 90$
0.8–1.0	$687 \pm 4 \pm 86$

tation functions [22] are used. The renormalization, factorisation and fragmentation scales are taken to be equal: $\mu = M = M_F = \xi p_t$ [2], with $\xi = 1$ for the central value. The scale uncertainty in the NLO calculation is estimated by varying the value of ξ from 0.5 to 2.0. The agreement with the data is poor in the high-p_t range for any choice of scale.

To test NLO QCD calculations in regions where non-perturbative subprocesses are better suppressed, we have also measured differential cross sections of $\pi^{\pm}$ production for $W_{\gamma\gamma} > 10$, 30 and 50 GeV. The results are shown in Table 4 and Fig. 4(b). The discrepancy between the calculations and data at high p_t is not significantly reduced by these stringent more $W_{\gamma\gamma}$ cuts.

Similar calculations were previously compared to γp reactions at HERA up to a p_t of 12 GeV and to $\bar{p}$p collisions up to a p_t of 20 GeV. Good agreement was found [23]. In the $\gamma\gamma$ channel, an excess of data with respect to NLO QCD was observed in tagged events at PETRA experiments [2]. No discrepancy is observed with the OPAL data which explore a p_t range up to 10 GeV. In this range, our data and the OPAL ones are well in agreement within the quoted uncertainties. A discrepancy with NLO QCD is revealed by our data which extend the measurement to higher p_t values.

References

[1] L.E. Gordon, Phys. Rev. D 50 (1994) 6753.
[2] J. Binnewies, B.A. Kniehl, G. Kramer, Phys. Rev. D 53 (1996) 6110.
[3] L3 Collaboration, P. Achard, et al., Phys. Lett. B 524 (2002) 44.
[4] L3 Collaboration, B. Adeva, et al., Nucl. Instrum. Methods A 289 (1990) 35;
M. Chemarin, et al., Nucl. Instrum. Methods A 349 (1994) 345;
M. Acciarri, et al., Nucl. Instrum. Methods A 351 (1994) 300;
G. Basti, et al., Nucl. Instrum. Methods A 374 (1996) 293;
I.C. Brock, et al., Nucl. Instrum. Methods A 381 (1996) 236;
A. Adam, et al., Nucl. Instrum. Methods A 383 (1996) 342.
[5] OPAL Collaboration, K. Ackerstaff, et al., Eur. Phys. J. C 6 (1999) 253.
[6] PYTHIA version 5.722 and JETSET version 7.409 are used with default options;
T. Sjöstrand, Comput. Phys. Commun. 82 (1994) 74.
[7] PHOJET version 1.05c is used with default options;
R. Engel, Z. Phys. C 66 (1995) 203;
R. Engel, J. Ranft, Phys. Rev. D 54 (1996) 4246.
[8] KK2f version 4.12 is used;
S. Jadach, B.F.L. Ward, Z. Wąs, Comput. Phys. Commun. 130 (2000) 260.
[9] KORALZ version 4.04 is used;
S. Jadach, B.F.L. Ward, Z. Wąs, Comput. Phys. Commun. 79 (1994) 503.
[10] KORALW version 1.33 is used;
M. Skrzypek, et al., Comput. Phys. Commun. 94 (1996) 216.
[11] F.A. Berends, P.H. Daverfeldt, R. Kleiss, Nucl. Phys. B 253 (1985) 441.
[12] R. Brun, et al., GEANT 3.15 preprint CERN DD/EE/84-1 (1984), revised 1987.
[13] H. Fesefeldt, RWTH Aachen report PITHA 85/2 (1985).
[14] P. Béné, et al., Nucl. Instrum. Methods A 306 (1991) 150;
D. Haas, et al., Nucl. Instrum. Methods A 420 (1999) 101.
[15] L3 Collaboration, M. Acciarri, et al., Phys. Lett. B 519 (2001) 33.
[16] R. Bizzarri, et al., Nucl. Instrum. Methods A 283 (1989) 799.
[17] G. D'Agostini, Nucl. Instrum. Methods A 362 (1995) 487.
[18] M.L. Perl, High Energy Hadron Physics, Wiley, 1974.
[19] B.A. Kniehl, private communication. We thank the author for providing us with NLO QCD calculations and for very usefull discussions.
[20] V.M. Budnev, et al., Phys. Rep. 15 (1974) 181.
[21] P. Aurenche, J.-P. Guillet, M. Fontannaz, Z. Phys. C 64 (1994) 621.
[22] B.A. Kniehl, G. Kramer, B. Pötter, Nucl. Phys. B 582 (2000) 514.
[23] B.A. Kniehl, G. Kramer, B. Pötter, Nucl. Phys. B 597 (2001) 337.